

Supplemental Information**Concerted action of CB1 cannabinoid receptor and Deleted in Colorectal Cancer (DCC) in axon guidance**

Abbreviated title: CB1R and RGC axon guidance

Anteneh Argaw^{1, 2}, Gabriel Duff^{2, 3}, Nawal Zabouri², Bruno Cécycy², Natacha Chainé², Hosni Cherif², Nicolas Tea², Beat Lutz⁴, Maurice Ptito² and Jean-François Bouchard^{2, 3}

¹Biomedical Sciences, Faculty of Medicine, University of Montreal, Montreal, Quebec, Canada, H3T 1J4

²School of Optometry, University of Montreal, Montreal, Quebec, Canada, H3T 1P1

³Faculty of Pharmacy, University of Montreal, Montreal, Quebec, Canada, H3C 3J7

⁴Institute of Physiological Chemistry, University Medical Center Mainz, Duesbergweg 6, 55128 Mainz, Germany

Corresponding author:

Jean-François Bouchard

School of Optometry, University of Montreal

3744, rue Jean-Brillant, Office- 260-7

Montreal, Quebec, Canada, H3T 1P1

Phone: (514) 343-6111 ext. 4083

Fax: (514) 343-2382

Email: Jean-Francois.Bouchard@umontreal.ca

Supplementary figure legends

Figure 1. Expression of the eCB system. *A*, primary cortical neurons immunolabeled for DAGL α , MGL and NFL. *B*, Western blot analysis of CB1R expression in primary neuron cultures at several DIVs. Molecular weight markers are indicated on the right side of the panel. *C*, Photomicrographs of retinal cross-sections showing CB1R, eCB synthesizing (NAPE-PLD, DAGL α) and eCB degrading (FAAH, MGL) enzyme expression (magenta) during early postnatal development. Syntaxin was used to label retinal projections (green). ONL, Outer nuclear layer; OPL, outer plexiform layer; INL, Inner nuclear layer; IPL, Inner plexiform layer; GCL, Ganglion cell layer; GCFL, Ganglion cell fiber layer. *D*, Photomicrographs of retinal tissues from CB1R^{-/-} and FAAH^{-/-} mice and matched wild type animals showing CB1R and FAAH antibodies specificity.

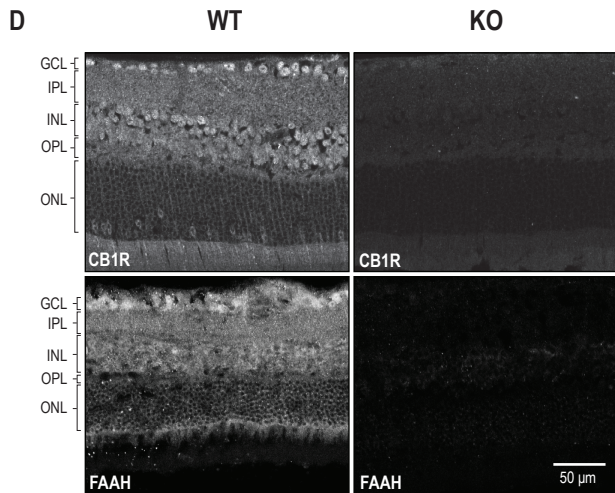
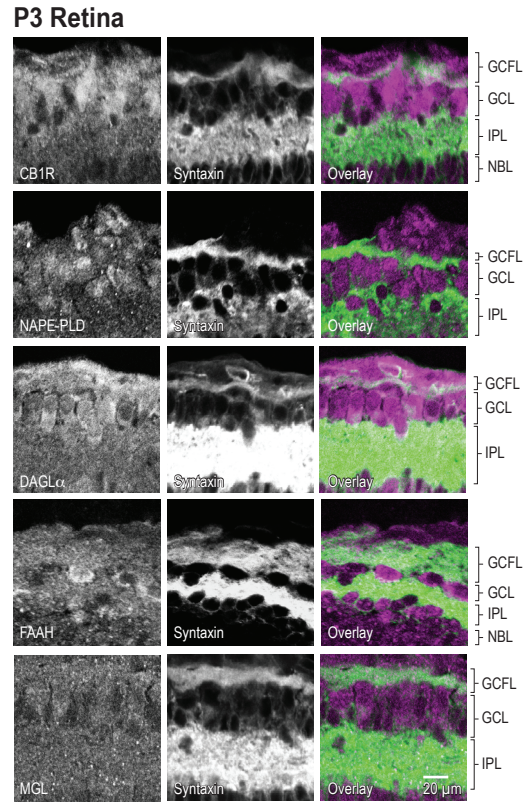
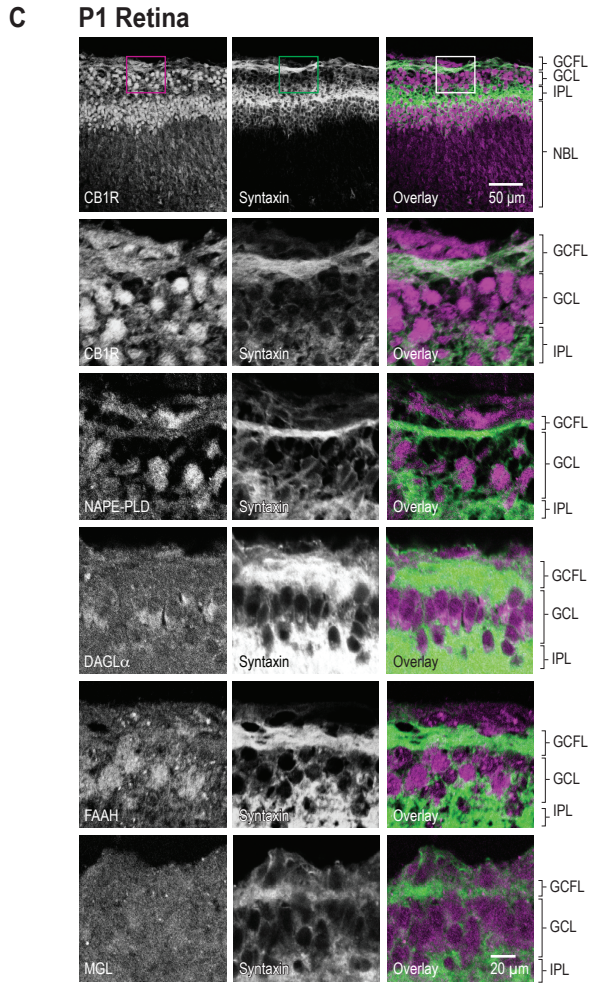
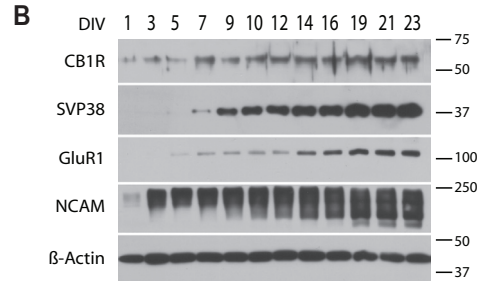
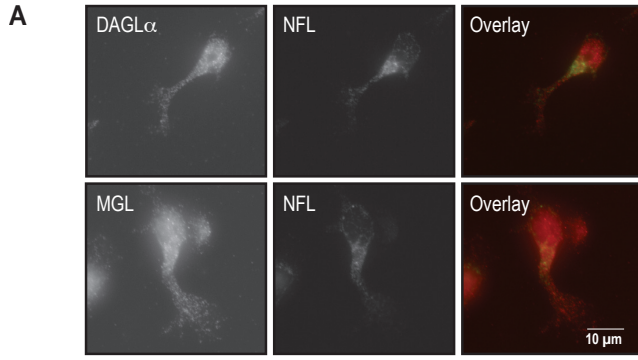
Figure 2. CB1R activity and second-messenger cascades. CB1R agonist, inverse agonist and antagonist did not activate the PI3K, ERK1/2 or mTOR pathways following a 20 min treatment (*A*). Molecular weight markers are indicated on the right side of the panel. Quantification of the optical density for P-AKT (*B*), P-ERK1/2 (*C*) and P-S6 (*D*). CB1R stimulation following KCl induced depolarisation (*E*) or insulin treatment (*F*) failed to recruit PI3K, ERK1/2 or mTOR second messenger cascades. Molecular weight markers are indicated on the right side of the panel.

Figure 3. DCC regulates CB1R induced reorganization of the GC. *A*, Photomicrographs of primary neuron cultures treated with α DCCfb followed by the

addition of either a CB1R inverse agonist or antagonist (AM251 or O2050, respectively) or FSK. GC photomicrographs of *dcc*^{-/-} (**B**) and *dcc*^{+/+} (**C**) primary neuron cultures treated with either ACEA or AM251.

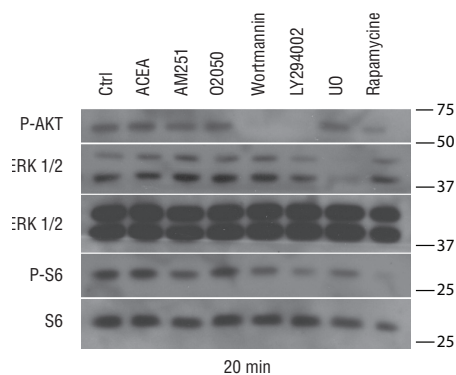
Figure 4. Intraocular injections and mechanism by which cannabinoids modulate GC steering. **A**, Schema illustrating vitreal injection and CB1R, FAAH and MGL expression analysis sites during retinal projection development. **B** and **C**, Illustrations of the methods used to quantify retinal projection branches length (**B**) and the number of retinal axon branches (**C**) in the DTN. Arrowed dotted lines indicate the distance between the lateral border of the thalamus and the tip of the farthest projections (**B**). **D**, Photomicrographs of optic nerves following vitreal injections of CTb-546 and CTb-488 in to the left and right eye, respectively. **E**, A model illustrating the interactions between the CB1R and DCC during axon navigation. Antagonizing the CB1R increases intracellular cAMP levels, triggering a PKA-dependent translocation of DCC to the plasma membrane and resulting in GC expansion, whereas CB1R agonists induce the opposite resulting in GC collapse.

Supplementary Figure 1

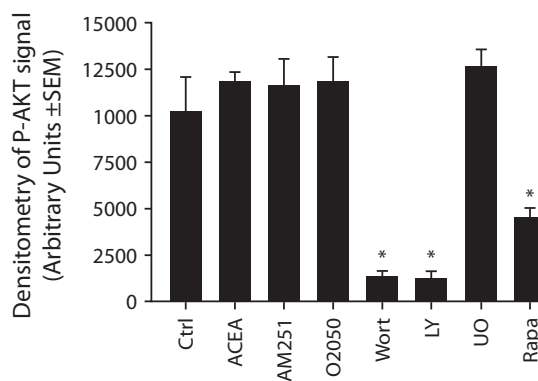


Supplementary Figure 2

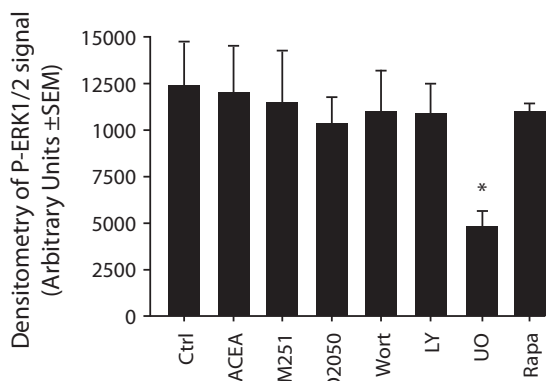
A



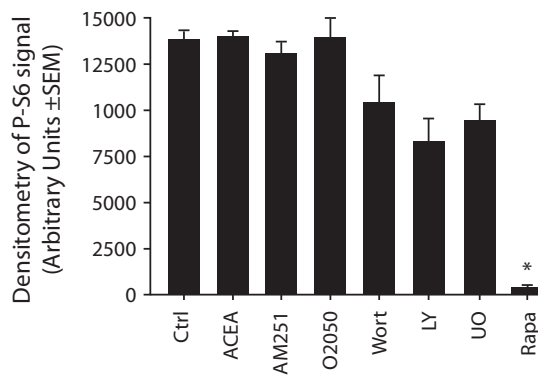
B



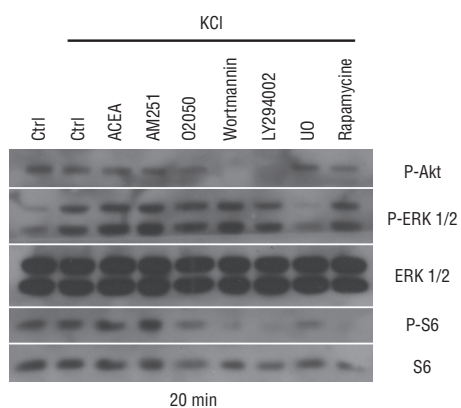
C



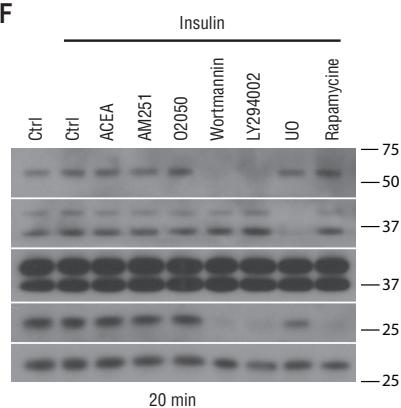
D



E

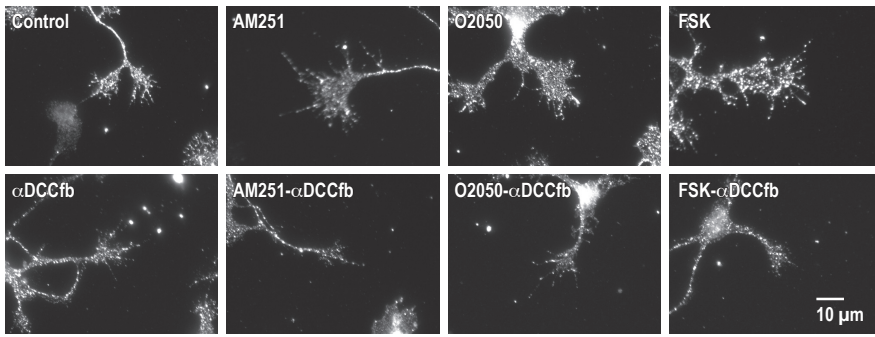


F



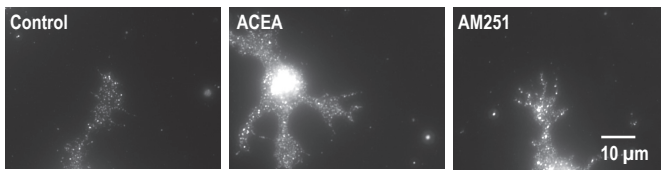
Supplementary Figure 3

A



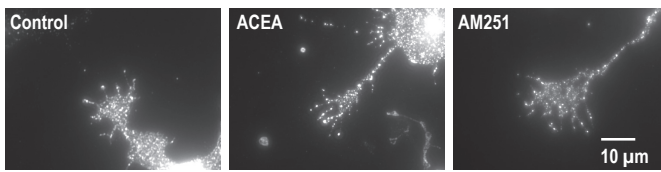
B

dcc^{-/-}



C

dcc^{+/+}



Supplementary Figure 4

